

Optical Coherence Tomography Evaluation of Tracheal Inflammation

¹Nevine Mikhail Hanna, ¹BS, Woong-Gyu Jung, MS, ¹Zhonping Chen, PhD,
¹Usama Mahmood, BS, ¹Reza Mina-Araghi, MD, ²Bryan Jordan, RN,
²Andrey Yershov, MD, PhD, ²Ronald Walton, DVM, ¹Matthew Brenner, MD.

¹Beckman Laser Institute
University of California, Irvine
1002 Health Sciences Road East
Irvine, CA 92612

²US Army Institute of Surgical Research
3400 Rawley E. Chambers Ave.
Fort Sam Houston
San Antonio, TX 78-234-6315

mbrenner@uci.edu
zchen@laser.bli.uci.edu

Supported by:
DOD: FA 9550-04-1-0101
Philip Morris: USA-32598

ABSTRACT

Background: Methods for obtaining real-time in-vivo histologic resolution non-invasive endoscopic optical imaging would be a major advance for pulmonary diagnostics and treatment in civilian and military medical applications. Optical coherence tomography (OCT) is a rapidly evolving technology based on near infrared interferometry that may provide these capabilities. **Purpose:** The purpose of this study is to evaluate the feasibility of using OCT for detecting airway pathology in a septic animal model. **Methods:** Tracheas of New Zealand white rabbits were inoculated endobronchially with varying concentrations of live *Streptococcus pneumoniae* bacteria. After development of pneumonia/sepsis, the animals were sacrificed. OCT tracheal images and subsequent histological preparations of these experimental animals were compared to control rabbit tracheas for morphological features and quantitative tracheal mucosal thicknesses measurements. **Results:** Results revealed significant airway mucosal thickening in the experimental group consistent with tracheal edema. Morphological changes, including epithelial sloughing and glandular proliferation, were evident in regions of the experimental tracheas. **Conclusions:** This study suggests that OCT is a potentially valuable imaging modality capable of evaluating superficial airway pathology with high resolution in-vivo. Numerous applications of OCT can be envisioned in the realm of combat casualty medicine and may substantially increase the precision and accuracy of current bronchoscopic diagnostic techniques.

KEYWORDS

Optical Coherence Tomography, imaging, airway, pneumonia, inflammation, edema.

Paper presented at the RTO HFM Symposium on "Combat Casualty Care in Ground Based Tactical Situations: Trauma Technology and Emergency Medical Procedures", held in St. Pete Beach, USA, 16-18 August 2004, and published in RTO-MP-HFM-109.

INTRODUCTION

Rapid and accurate evaluation of airway pathologic changes is paramount for minimizing morbidity and mortality in conditions such as acute burn or inhalation injury¹⁻⁷. Until now, assessment for proper clinical management relied primarily on visualization of abnormalities, during endoscopic biopsy or on frozen sections sent to pathology, and gross inspection at surgery. A means to obtain real-time non-invasive histologic imaging would aid in diagnosis, prognosis, and help to ensure higher yield biopsy samples, save operating time, and may also help avoid unnecessary interventions or repeated procedures.

Optical Coherence Tomography (OCT) is emerging as a new rapid acquisition high-resolution imaging modality that provides capabilities for real-time near histologic level evaluation⁸. In attempting to approach the concept of “optical biopsy”⁹, OCT offers the potential for surface and subsurface optical imaging (up to a depth of 1-3 mm) with high spatial resolution of tissue microstructure, without requiring contact between the optical probe and the tissue sample^{9 10-12}. Tissue layers, glands, small blood vessels, and cartilage can be visualized with resolutions approaching 10 micrometers with the use of superluminescent diode (SLD) laser prototype systems^{13 14,15}. These technologies, in combination with minimally invasive techniques, can be applied in combat casualty care to evaluate and examine tissue depth and level of injury, provide prognostic information, as well as a means to assess response to therapy, and potentially minimize the need for frozen sections or the uncertainties associated with gross examination^{16 17 18,19}.

The purpose of this study was to investigate the potential utility of OCT in detecting airway pathology in acute injury. In order to demonstrate this concept, an animal model of airway disease was employed in which the airways of rabbits were inoculated with live *Streptococcus pneumoniae* bacteria. Previous studies with animals have found that bacterial lung infection—and specifically infection with pneumococcus—induces an inflammatory process within the airways. Thus, it was hypothesized that minimally invasive OCT imaging of tracheas of *S. Pneumonia* infected rabbits, would reveal morphological changes indicative of airway inflammation when compared to those of controls.

MATERIALS AND METHODS

SLD OCT Prototype

Optical coherence tomography theory has been discussed in detail in previous studies^{14,20-33}. Briefly, OCT uses a broadband near-infrared laser light source in which the emitted light is split into sample and reference beams. The sample beam is directed to the tissue being examined, which is reflected back and combined with the reflected reference beam that has travelled an equal distance from a reference mirror to create an interference pattern (Fig 1). The interference signal of the resultant light wave (a combination of the reflected sample and reference beam) is processed and translated digitally as a gray-scale or false-color map. The reflected signals at different axial tissue depths are determined by the comparison of the internal tissue surface reflected distances and the reference mirror as the mirror distance (delay line) is increased and decreased. The tissue sampling arm probe is then moved laterally, thereby creating a two dimensional image.

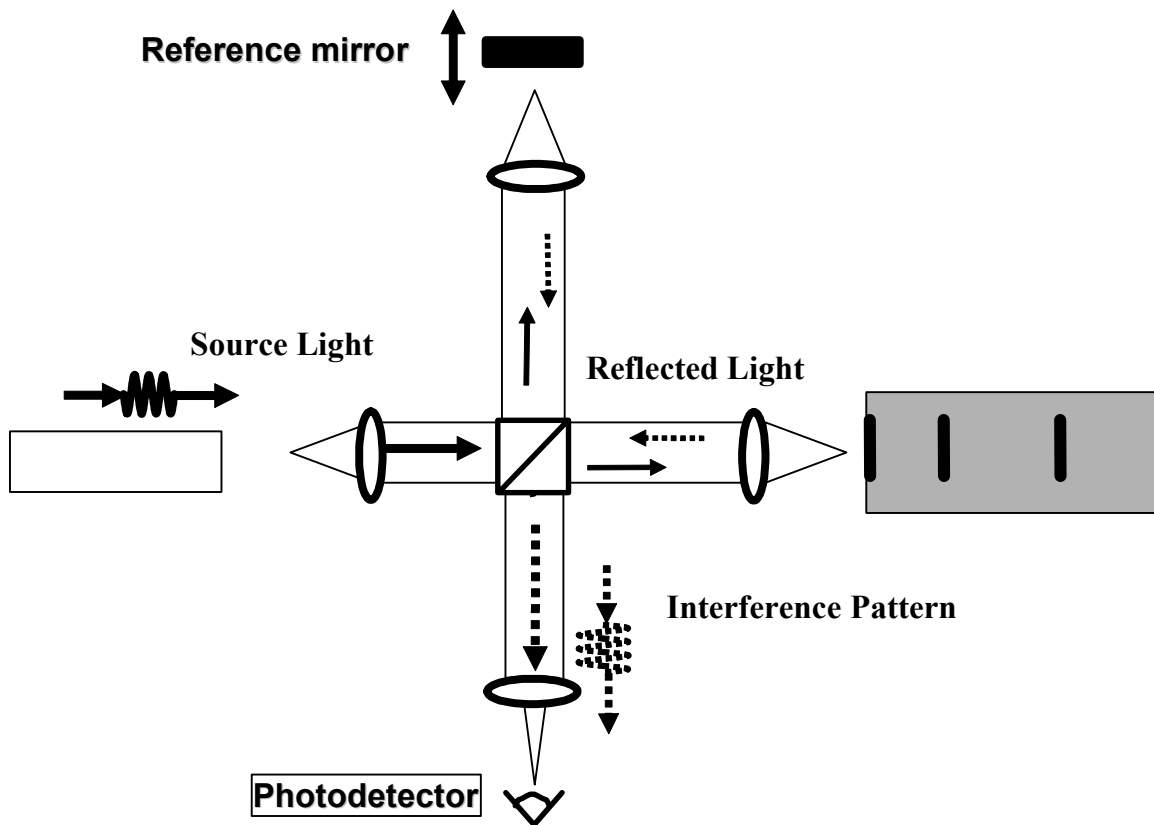


Figure 1: OCT Experimental Setup: Light Reflection Imaging Principle: Light is Emitted from the Low Coherence Laser Source, Travels to the Target Tissue and is Reflected Off the Surface at Various Depths. The Incident and Reflected Waves Combine to Create an Interference Pattern, Indicating the Depth of the Measured Internal Tissue Reflecting Surface.

A simplified diagram of the OCT system we constructed in our laboratory is shown in figure 2. A low temporal coherence superluminescent diode light source (central wavelength $\lambda_0 = 1300\text{nm}$, FWHM $\Delta 80\text{nm}$; AFC Technologies Hull, Quebec) was connected to a Michelson interferometer which split the light source into the sample and reference beams. These reflected beams were then recombined at the fiber coupler in the interferometer, producing an interference pattern that was detected by a photodiode. Signal processing and data acquisition was accomplished using a computer. Cross sectional images were constructed by repeating the measurements at adjacent lateral points along a sampling line. Axial line scan frequency was 500 Hz. Imaging depth was approximately 1~2 mm. Since the OCT light source is not visible, an aiming beam (laser diode with $\lambda=650\text{nm}$) was coupled to the system to elucidate the exact location of the sampling site.

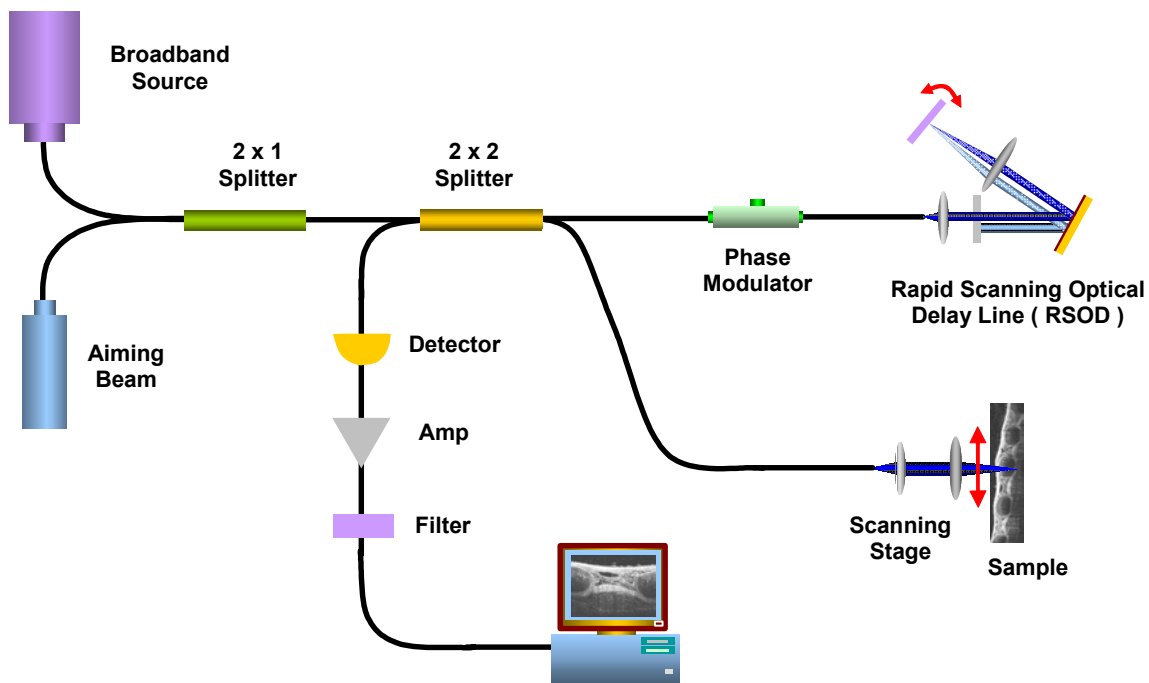


Figure 2: OCT Schematic. A schematic depicting the design of the superluminescent diode OCT prototype system used for these studies. Returning light is recombined at the partially reflecting mirror and read the photodetector. Results are processed and displayed. The light source of 1310nm broad band super-luminescent diode with 50 nm bandwidth (FWHM), and theoretical resolution of 10~15 μ m.

Animal Models

Airway Inhalation Injury Induction. 23 New Zealand white rabbits were inoculated with various quantities of *S. pneumoniae* $1.9 \times 10^3 - 2.4 \times 10^5$ cells using a sterile pediatric suction catheter on an approved protocol from the Institute of Surgical Research in San Antonio, TX. Animals were monitored at the time of exposure and 24, 48, 72 and 96 hours post exposure via blood work, pulmonary function tests, vital sign data, computerized tomography scans, and flow cytometry and cultures of bronchoalveolar lavage fluid to confirm diagnosis of pneumonia. On the fourth day following inoculation, surviving rabbits were sacrificed and their tracheas excised, placed in isotonic saline packed on ice and sent overnight to the Beckman Laser Institute. Effort was made to image all specimens as soon as possible, within two days of excision.

The normal control group consisted of 9 total tracheal specimens. Six tracheal specimens that underwent the same process as the septic tracheas without the inoculation with the *S. pneumoniae*. Another 3 specimens were obtained as part of an unrelated study to evaluate acute hemorrhagic shock hemodynamics. The hemorrhagic shock specimens were used to evaluate whether time lapsed when the tracheas are stored in saline affected the structure of the trachea. Successive amounts of blood were removed and replaced with saline within a three-hour period. At the completion of these experiments, the rabbits were sacrificed and their tracheas removed and maintained in isotonic saline and imaged on site at the Beckman Laser Institute on the campus of the University of California at Irvine. In the saline stored control group, the tracheas were harvested. The tracheas were imaged immediately after resection, then stored in saline. Serial OCT images were obtained daily up to 4-5 days post resection to note the effects of saline storage on tracheas mucosal, submucosa.

Optical Coherence Tomography Imaging

Ex-Vivo Tracheal OCT. Excised tracheas were cut open longitudinally along their musculofibrous membranes and divided into approximately 2 cm-long sections, each tracheal specimen yielded two samples, representing upper and lower trachea. Triangular notches were cut into opposite ends of each specimen to delineate the line of image acquisition, perpendicular to the cartilage rings. The tracheas were secured to pieces of cork using metal pins placed along their perimeter and covered by a layer of KY jelly to prevent desiccation during imaging (Figure 3). The tracheas were then placed on a moveable sample platform and a visible-light guiding beam was used to match the line of image acquisition with the triangular marking notches. The images constructed were displayed using a logarithmic intensity scale with the most backscattering areas represented in white and the least backscattering areas in black. The trachea was then prepared for standard H&E slides for comparison to the OCT images.



Figure 3: Excised tissue set up for OCT imaging.

Histology

Histology of excised tissue was prepared according to standard hematoxylin and eosin (H&E) histological staining method. OCT images and those of the histological sections were compared. Tissue slide examination and micrographs were performed with an Olympus BH2 light microscope (Olympus American, Melville, NY), and recorded using an Olympus DP10 camera (Olympus American, Melville, NY) for a light microscope and Olympus Digital Microfire 1.0 (Olympus American, Melville, NY).

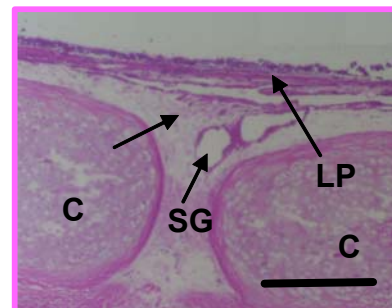
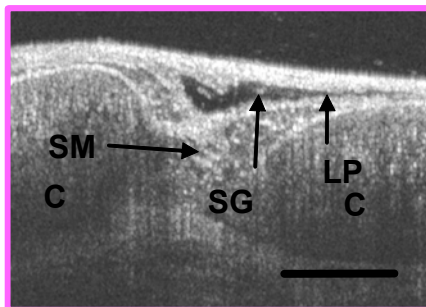
RESULTS

We constructed a compact prototype OCT unit, which was capable of performing cross-sectional imaging with an axial and transverse resolution of 10-20 μm in complex airway tissues. 14 mm x 1.3 mm airway images were acquired and displayed in near “real-time” on a computer screen. High-resolution images of normal and diseased trachea were obtained using OCT. These images revealed levels of resolution capable of clearly identifying airway structures.

OCT images and the corresponding histology sections are shown in figures 4 for both normal and inflamed trachea. Trachea cartilage (C) was an identifiable landmark seen in OCT imagining which was confirmed with histology. OCT images were able to distinguish the submucosa (SM) from the lamina propria (LP). Also observed in both OCT mapping and histology sections were submucosal glands between cartilage rings (B). A slight variation in tissue structure occurred, with decreased submucosal layer thickness in the histologic specimens, which was believed to have resulted from tissue desiccation changes after excision and fixation. Injured trachea obtained from animals inoculated with *S. pneumoniae* demonstrated a thickened submucosa that was seen in both OCT imagining and histology.

Normal vs. Septic Inhalation Injury Trachea

Normal trachea



ISR trachea

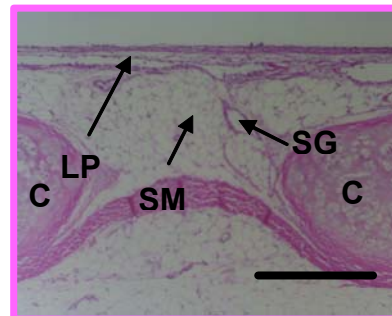
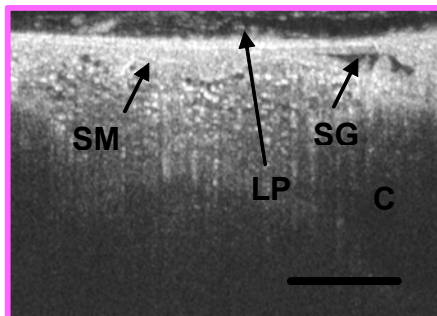


**Figure 4: Top - Normal control trachea OCT (left) and corresponding standard H&E histology (right)
Bottom - Inhalational injury (ISR) trachea OCT (left) and its corresponding standard H&E histology (right). Note the thickness of the submucosa as compared to control. Structural elements are clearly seen in corresponding images. (C – tracheal cartilage; SM – submucosa; LP – lamina propria B – cartilage rings; G – submucosal glands).**

The average tracheal mucosal layer thickness above the cartilage rings for the control group was 150 +/- 2.5 um micrometers whereas that for the pneumonia group was 228 micrometers +/- 1.7 um). There was a significant difference ($p < 0.005$) between the infected mucosal thicknesses and the thicknesses from the other two control groups. There was no difference between the values obtained from the control hemorrhage vs intubated control animals ($p = 0.50$). A dose-response curve shows a weak correlation between the increase in mucosal thickness with dosage of S Pneumoniae inoculated (Figure 5). There was no significant difference in upper versus lower tracheal specimens, and storing the tracheal sample in saline for several days had no impact on image appearance or the thickness of the mucosal and submucosal layers.

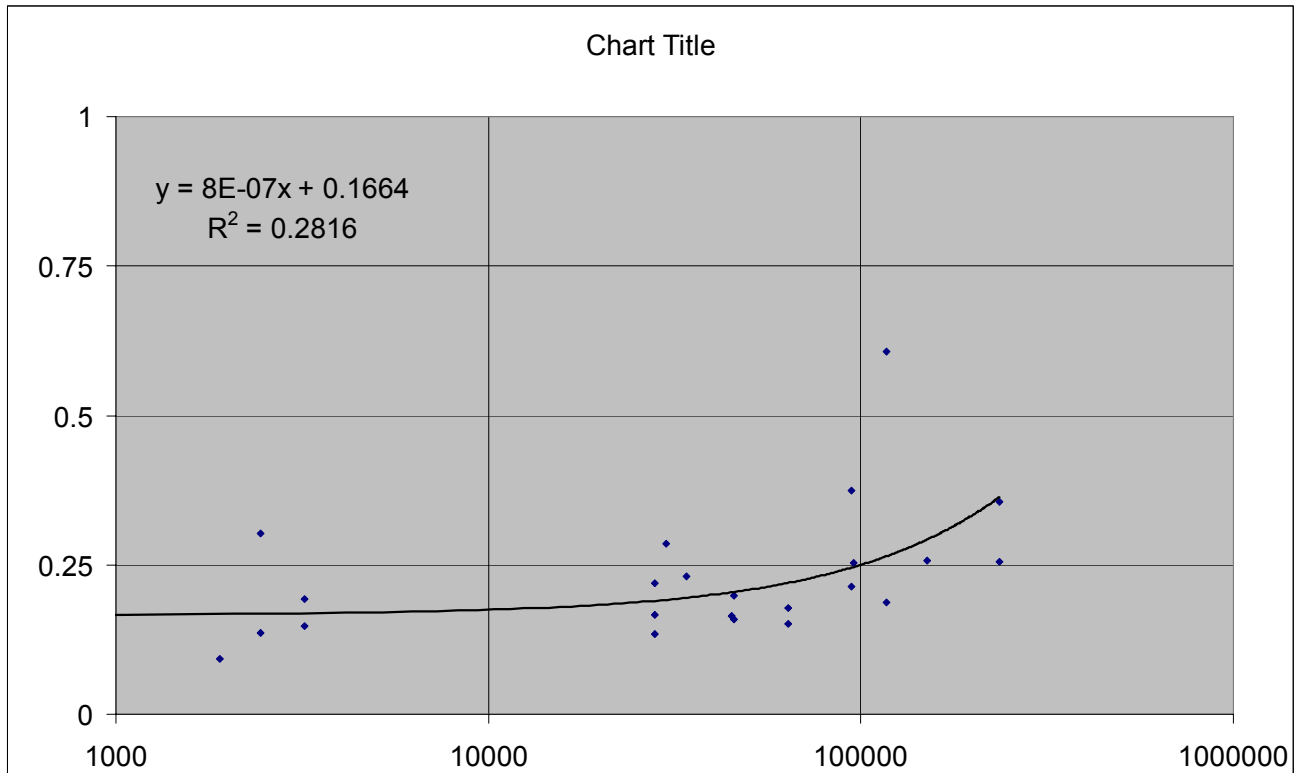


Figure 5: Dose response curve for septic tracheal mucosal thickness.

DISCUSSION

These studies confirm the feasibility of high resolution OCT imaging of airway to obtain optical images at near histologic level in-vivo. Differences in tissue layers of the airway were clearly distinguishable and corresponded closely to standard H&E images subsequently obtained from the excised tissues.

Studies in our lab have also demonstrated OCT capabilities in upper airway in ex-vivo specimens. There are many areas of combat casualty airway and thoracic clinical diagnostics and research where OCT may become useful as resolution improves. With availability of in-vivo high-resolution optical capabilities, responses to therapy in thoracic injuries and diseases might be better assessed in addition to more rapid and improved diagnostics. At the current level of resolution (10-20um), tissue layers, mucosa, and airway epithelium can be readily visualized. Architectural disruptions in diseased tracheal specimens (Fig 4) clearly demonstrated an

Optical Coherence Tomography Evaluation of Tracheal Inflammation

increase in mucosal thickness that suggested tissue damage. Structural changes can also be observed in acute airway injury, which could make the use of the current OCT technology with bronchoscopy valuable in the acute trauma setting. In airway burn and toxic inhalation injuries, delineation of submucosal edema, hyperemia, and blood flow changes by OCT (including use of Optical Doppler Tomography (ODT) techniques)³⁴⁻⁴⁴ could be a significant adjunct to bronchoscopy for the management of tracheal and bronchial injury and assessment of response to therapy.

The ability to visualize tissue structures in real-time at a near histologic level resolution opens up a wide range of potential areas for clinical and research applications for injured soldiers. In the future, when cellular level OCT resolutions are obtained, even greater uses for OCT in thoracic diagnostic can be envisioned. However, the depth of penetration of OCT is relatively shallow (1-3 millimetres) and is likely to remain limited by the degree of scattering inherent in complex biological tissues of the lung and thorax (thus, major advances in depth of penetration are unlikely). Nevertheless, there are many scenarios in combat casualty medicine in which surface and near surface high-resolution imaging are of great potential value.

The development of three-dimensional high-resolution OCT probes, endoscopes, and image processing and display technologies may allow for improved assessment of tissue injury. Further into the future, very small OCT probes could be designed to fit within needles to allow imaging at depths within tissues and organs with near real-time histologic resolution capabilities.

SUMMARY

This study has demonstrated the feasibility of high-resolution OCT for examination of airway injury. The current technology is limited to 10-20um resolutions, and maximum depth of penetration is generally 2-3 mm. With further improvement in resolution, contrast, acquisition, display and processing, and development of specific thoracic probes, OCT may offer a significant advance for the diagnosis and treatment of patients with burn and toxic inhalational injury as well as other airway pulmonary diseases.

ACKNOWLEDGEMENTS:

We would like to thank Teri-Waite, David Mukai, Sugku Han, and Tanya Burney for their technical assistance.

REFERENCES

- [1] Hunt JL, Agee RN, Pruitt BA, Jr. Fiberoptic bronchoscopy in acute inhalation injury. *J Trauma* 1975; 15:641-649
- [2] Bang RL, Sharma PN, Sanyal SC, et al. Septicaemia after burn injury: a comparative study. *Burns* 2002; 28:746-751
- [3] Ribeiro CA, Andrade C, Polanczyk CA, et al. Association between early detection of soluble TNF-receptors and mortality in burn patients. *Intensive Care Med* 2002; 28:472-478
- [4] Skuba ND, Strekalovskii VP, Ustinova TS, et al. [Thermal trauma in a combination with respiratory tract burn]. *Khirurgiia (Mosk)* 2000:37-40

- [5] Nylen ES, O'Neill W, Jordan MH, et al. Serum procalcitonin as an index of inhalation injury in burns. *Horm Metab Res* 1992; 24:439-443
- [6] Paul S, Bueno R. The burned trachea. *Chest Surg Clin N Am* 2003; 13:343-348
- [7] Polverosi R, Vigo M, Baron S, et al. [Evaluation of tracheobronchial lesions with spiral CT: comparison between virtual endoscopy and bronchoscopy]. *Radiol Med (Torino)* 2001; 102:313-319
- [8] Reiss SM. *Optical Coherence Tomography, An Imaging Modality for the New Millennium*. Biophotonics International 1999
- [9] Tadrous PJ. Methods for imaging the structure and function of living tissues and cells: 2. Fluorescence lifetime imaging. *J Pathol* 2000; 191:229-234
- [10] Tanno N, Kishi S. Optical coherence tomographic imaging and clinical diagnosis. *Medical Imaging Technology* 1999; 17:3-10
- [11] Swanson EA. *Optical coherence tomography: principles, instrumentations, and applications*, 1999; 312
- [12] Swanson EA, Hee MR, Tearney GJ, et al. Application of optical coherence tomography in nondestructive evaluation of material microstructure, 1996; 326-327
- [13] Chen W, Xue P, Yuan T, et al. Optical coherence tomography system with SLD and ultrashort pulse laser. *Chinese Journal of Quantum Electronics* 2000; 17:360-364
- [14] Kulkarni MD, Izatt JA. Spectroscopic optical coherence tomography, 1996; 59-60
- [15] Hitzenberger CK, Danner M, Drexler W, et al. Measurement of the spatial coherence of superluminescent diodes. *Journal of Modern Optics* 1999; 46:1763-1774
- [16] Yingtian P, Lavelle JP, Bastacky SI, et al. Detection of tumorigenesis in rat bladders with optical coherence tomography. *Medical Physics* 2001; 28:2432-2440
- [17] Park BH, Saxer C, Srinivas SM, et al. In vivo burn depth determination by high-speed fiber-based polarization sensitive optical coherence tomography. *J Biomed Opt* 2001; 6:474-479
- [18] Marsack J, Ducros M, Parekh S, et al. Imaging the primate retina using polarization sensitive optical coherence tomography, 2001; 158-163
- [19] Amelinckx S, van Dyck D, van Landuyt J, et al. *Handbook of microscopy. Applications in materials science, solid-state physics and chemistry. Methods I*. 1997
- [20] Hrynchak P, Simpson T. *Optical coherence tomography: an introduction to the technique and its use*. *Optometry and Vision Science* 2000; 77:347-356
- [21] Izatt JA, Rollins AM, Ung-Arunyawee R, et al. Real-time endoscopic optical coherence tomography in human patients, 1999; 336-337
- [22] Schmitt JM. Optical coherence tomography (OCT): a review. *IEEE Journal of Selected Topics in Quantum Electronics* 1999; 5:1205-1215

Optical Coherence Tomography Evaluation of Tracheal Inflammation

- [23] Fujimoto JG. Biomedical imaging using optical coherence tomography, 1998; 51
- [24] Fujimoto JG. Biomedical imaging using optical coherence tomography, 1999; 402-403
- [25] Hansen KA, Barton JK, Weiss JA. Optical coherence tomography imaging of collagenous tissue microstructure, 2000; 581-587
- [26] Bouma BE, Tearney GJ. Clinical imaging with optical coherence tomography. *Acad Radiol* 2002; 9:942-953
- [27] Fujimoto JG, Bouma BE, Tearney GJ, et al. Optical coherence tomography for biomedical imaging and diagnostics, 1997; 2-6
- [28] Fujimoto JG, Drexler W, Li XD, et al. Optical coherence tomography for biomedical imaging, 2000; 656-658
- [29] Fujimoto JG, Drexler W, Morgner U, et al. Optical coherence tomography: high resolution imaging using echoes of light. *Optics & Photonics News* 2000; 11:24-31
- [30] Fujimoto JG, Pitris C, Boppart SA, et al. Optical coherence tomography: an emerging technology for biomedical imaging and optical biopsy. *Neoplasia* 2000; 2:9-25
- [31] Fujimoto JG. Optical coherence tomography. *Comptes Rendus de l'Academie des Sciences, Serie IV (Physique, Astrophysique)* 2001; 2:1099-1111
- [32] Swanson EA, Chinn SR, Boppart SA, et al. Optical coherence tomography: principles, instrumentation, and applications, 1996; 125-128
- [33] Thrane L, Andersen PE, Jorgensen TM, et al. Optical coherence tomography. *Dops-Nyt* 2001; 16:13-18
- [34] Kajiya F. Progress and recent topics in blood flow measurements. *Front Med Biol Eng* 1989; 1:271-285
- [35] Machens HG, Mailaender P, Rieck B, et al. Techniques of postoperative blood flow monitoring after free tissue transfer: an overview. *Microsurgery* 1994; 15:778-786
- [36] Chen Z, Milner TE, Wang X, et al. Optical Doppler tomography: imaging in vivo blood flow dynamics following pharmacological intervention and photodynamic therapy. *Photochem Photobiol* 1998; 67:56-60
- [37] Lindmo T, Smithies DJ, Chen Z, et al. Accuracy and noise in optical Doppler tomography studied by Monte Carlo simulation. *Phys Med Biol* 1998; 43:3045-3064
- [38] Kehlet Barton J, Izatt JA, Kulkarni MD, et al. Three-dimensional reconstruction of blood vessels from in vivo color Doppler optical coherence tomography images. *Dermatology* 1999; 198:355-361
- [39] Jones M, Berwick J, Johnston D, et al. Concurrent optical imaging spectroscopy and laser-Doppler flowmetry: the relationship between blood flow, oxygenation, and volume in rodent barrel cortex. *Neuroimage* 2001; 13:1002-1015
- [40] Rollins AM, Yazdanfar S, Barton JK, et al. Real-time in vivo color Doppler optical coherence tomography. *J Biomed Opt* 2002; 7:123-129

- [41] Wong RC, Yazdanfar S, Izatt JA, et al. Visualization of subsurface blood vessels by color Doppler optical coherence tomography in rats: before and after hemostatic therapy. *Gastrointest Endosc* 2002; 55:88-95
- [42] Chang CJ, Hou KH. High-resolution optical Doppler tomography for in vitro and in vivo fluid flow dynamics. *Chang Gung Med J* 2003; 26:403-411
- [43] Leitgeb RA, Schmetterer L, Hitzenberger CK, et al. Real-time measurement of in vitro flow by Fourier-domain color Doppler optical coherence tomography. *Opt Lett* 2004; 29:171-173
- [44] Schaefer AW, Reynolds JJ, Marks DL, et al. Real-time digital signal processing-based optical coherence tomography and Doppler optical coherence tomography. *IEEE Trans Biomed Eng* 2004; 51:186-190

